High resolution infrared spectroscopy of H12C13CD and H13C12CD: The bending states up to v4 + v5 = 2

5 AUTHORS, INCLUDING:

Filippo Tamassia
University of Bologna
72 PUBLICATIONS **473** CITATIONS

SEE PROFILE

Gianfranco Di Lonardo
University of Bologna
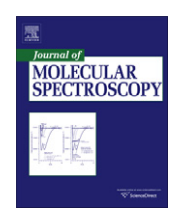**145** PUBLICATIONS **1,790** CITATIONS

SEE PROFILE

High resolution infrared spectroscopy of H^{12}C^{13}CD and H^{13}C^{12}CD: The bending states up to $v_4 + v_5 = 2$

L. Fusina [a,*], E. Canè [a], F. Tamassia [a], A. Baldan [b], G. Di Lonardo [a]

[a] Dipartimento di Chimica Fisica e Inorganica, Università di Bologna, Viale Risorgimento 4, I-40136 Bologna, Italy
[b] Dipartimento di Scienze Molecolari e Nanosistemi, Università Cá Foscari di Venezia, Calle Larga Santa Marta 2137, I-30123 Venezia, Italy

ARTICLE INFO

ABSTRACT

The high-resolution infrared spectrum of two partially deuterated isotopologues of acetylene, H^{12}C^{13}CD and H^{13}C^{12}CD, has been recorded by Fourier transform spectroscopy in the range 450–1850 cm^{-1}. The bending fundamental bands and a number of overtone, combination and hot bands have been identified for both isotopomers. In total, 17 vibrational bands for H^{12}C^{13}CD and 18 bands for H^{13}C^{12}CD were analyzed, involving all the *l*-vibrational components of the excited bending states up to $v_t = v_4 + v_5 = 2$. The data pertaining to each molecule were analyzed together with the pure rotational transitions recorded in the millimeter- and sub-millimeter-wave frequency ranges and the $v_5 \leftarrow v_4$ band available in the literature. The model Hamiltonian adopted for the analysis takes into account the usual vibration and rotation *l*-type resonances. The ground state and 9 vibrationally excited states have been characterized for each isotopomer. The spectroscopic parameters obtained from the fits reproduce 1617 transitions for H^{12}C^{13}CD and 1613 transitions for H^{13}C^{12}CD, with standard deviations of the fit equal to 0.00038 cm^{-1} and 0.00032 cm^{-1}, respectively.

© 2011 Elsevier Inc. All rights reserved.

1. Introduction

Partially deuterated acetylene isotopologues have been recently the subject of several spectroscopic investigations. They are interesting owing to the fact that the bending and stretching vibrationally excited states at low energy are not perturbed by anharmonic interactions affecting the symmetric fully hydrogenated or deuterated acetylenes. The analysis of their infrared (IR) spectra thus provides unperturbed parameters, which represent useful information for the determination of the anharmonic force field of acetylene. Differently from the symmetric isotopologues, the presence of a very small dipole moment allows the observation of pure rotational transitions, which complement the ground state combination differences from IR data to obtain accurate values for the ground state parameters.

^{12}C$_2$HD has been the most studied molecule, also as a consequence of its detection in Titan's atmosphere by the CIRS instrument mounted on CASSINI spacecraft [1,2]. Besides the ground state, bending states up to $v_t = v_4 + v_5 = 3$ have been accurately characterized through the analysis of a large number of IR and far infrared (FIR) bands, including fundamentals, overtones, combination and hot bands in addition to rotational transitions [3–5].

^{13}C$_2$HD has been the subject of less numerous IR studies, leading however to the characterization of the same set of states as in ^{12}C$_2$HD [6].

In case of H^{12}C^{13}CD and H^{13}C^{12}CD, only the first vibrationally excited state of the bending modes and the Σ^+ components of the $v_4 = 2$, $v_5 = 2$, and $v_4 = v_5 = 1$ manifolds have been investigated [7,8]. In fact, transitions of the two species were identified as impurity in the spectra of H^{13}C^{12}CH or in natural abundance in the spectra of ^{12}C$_2$HD. In addition, rotational transitions in the millimeter and sub-millimeter wave regions provided accurate values of the rotational and centrifugal distortion constants [4].

Here we present a high resolution study of all the bending states up to $v_t = 2$ for H^{12}C^{13}CD and H^{13}C^{12}CD. A sample containing higher concentrations of the two species, as compared to those present in previous recordings, has been synthesized. The spectra were measured in the range 450–1450 cm^{-1} using a sample containing about 20% of H^{12}C^{13}CD and 20% of H^{13}C^{12}CD. Interfering bands due to D^{13}C^{12}CD, H^{13}C^{12}CH, and H$_2$^{13}C^{12}CH$_2$ were present in the observed spectra. In addition, the $v_5 \leftarrow v_4$ hot band centered at 166.36 cm^{-1} for H^{12}C^{13}CD and 157.68 cm^{-1} for H^{13}C^{12}CD cm^{-1} has been identified as an impurity in the FIR spectrum of ^{12}C$_2$HD [5].

The identification and the analysis of transitions involving all the components of the manifolds with double excitation of the bending modes provide accurate information on the vibrationally excited states, in particular of those not observed in previous studies. This allows the determination of rotational and vibrational

l-type resonance parameters, and of the anharmonicity constants for the bending modes, together with the improvement of the spectroscopic parameters reported in the literature. The obtained results will give a better insight into the isotopic dependence of the parameters characterizing the bending states for all the acetylene isotopologues.

2. Experimental details

A sample constituted by $D^{13}C^{12}CD$, $H^{12}C^{13}CD$, $H^{13}C^{12}CD$ and $H^{13}C^{12}CH$ was obtained by modifying a synthetic method for $[1-^{13}C]$ acetylene [9]. The reaction sequence is summarized as

$$[Si(CH_3)_3]_2NLi \xrightarrow[\substack{1.BrH_2{}^{12}C^{13}CH_2Br \\ 2.CH_3CO_2D}]{} \underset{\sim30\%}{D^{13}C^{12}CD} + \underset{\sim20\%}{H^{12}C^{13}CD}$$
$$+ \underset{\sim20\%}{H^{13}C^{12}CD} + \underset{30\%}{H^{13}C^{12}CH}$$

The precursor $BrH_2{}^{12}C^{13}CH_2Br$ was prepared starting from $^{12}CH_3{}^{13}CH_2OH$ (99% atom ^{13}C, CortecNet) as detailed in [10]. Lithium bis(trimethylsilyl) amide, $[Si(CH_3)_3]_2NLi$, (1.0 M solution in THF) and deuterated acetic acid, CH_3CO_2D, (99% atom D) were obtained by Sigma–Aldrich. The overall yield of $[1-^{13}C]$ acetylene isotopologues, on a 20 mmol scale, was ∼73%.

Several high resolution IR spectra of the above described mixture were recorded with a BOMEM DA3.002 FT interferometer at the University of Bologna under different experimental conditions. For the region 450–1000 cm^{-1} the interferometer was equipped with KBr beam splitter, Globar source, and a HgCdTe detector. An optical path length of 0.18 m was adopted with sample pressures of 130 Pa and 1300 Pa. For the low pressure spectrum the attained unapodized resolution was 0.004 cm^{-1}. A very large number of scans (880) were co-added in order to improve the S/N ratio below 550 cm^{-1}. In the case of the 1300 Pa sample the interferograms were recorded up to a maximum optical path difference of 165 cm to give an instrument unapodized function with a full width at half maximum of 0.006 cm^{-1}. The attained resolution was 0.0078 cm^{-1}.

The spectra recorded in the 950–1850 cm^{-1} region were obtained with the same resources as described above, but a different HgCdTe detector was adopted, with a detectivity D^* about 50 times larger than that used in the low wavenumber region. Rovibrational transitions of H_2O [11] present inside the interferometer and of NH_3 [12], present as an impurity, were used for calibration. The wavenumber accuracy and precision of the measured transitions were estimated to be about 0.0002 cm^{-1}.

3. Results and discussion

The spectrum appears very congested due to the presence of transitions belonging to four different isotopologues at about the same concentration. The identification of transitions for the partially deuterated species was facilitated by the accurate knowledge of the $H^{13}C^{12}CH$ [10] and $D^{13}C^{12}CD$ [13] bands in the investigated region. Moreover, the bending fundamentals and some overtones and combination bands for the studied molecules have been already reported [8].

Figs. 1 and 2 illustrate the regions of the bending fundamentals from the spectra recorded with a sample pressure of 130 Pa at a resolution of 0.004 cm^{-1}. The *Q*-branches of the ν_4 and ν_5 fundamental bands for both isotopomers are shown in Figs. 1 and 2, respectively. The spectral region containing ν_4 has a S/N ratio lower than the rest of the spectrum because of the poor performance of our HgCdTe detector below 550 cm^{-1}. However, the improvement in the S/N ratio of the spectrum presently recorded is evident by comparing Fig. 1 to the analogous figure in
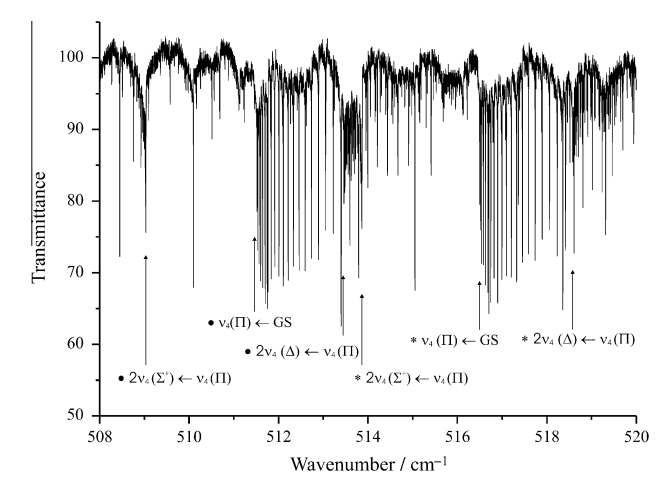

Fig. 1. The *Q*-branch of the $\nu_4 \leftarrow$ GS band for $H^{12}C^{13}CD$ (●) and $H^{13}C^{12}CD$ (*) and related hot bands. Experimental conditions: pressure 133 Pa, absorption path length 0.18 m, resolution 0.004 cm^{-1}, acquisition time 84 h.

Fig. 2. The *Q*-branch of the $\nu_5 \leftarrow$ GS band for $H^{12}C^{13}CD$ (●) and $H^{13}C^{12}CD$ (*) and related hot bands. Experimental conditions: pressure 133 Pa, absorption path length 0.18 m, resolution 0.004 cm^{-1}, acquisition time 84 h.
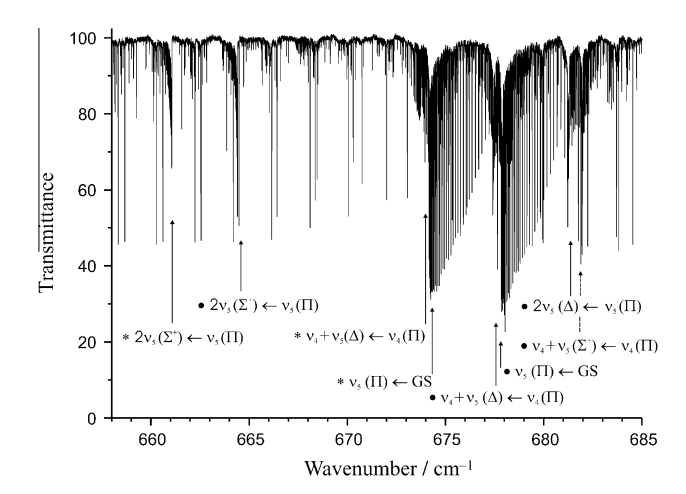
[8]. Transitions of the ν_4 and ν_5 bands previously observed [8] were first identified, extending the *J* ranges of the *P*, *Q*, and *R* branches.

Table 1 collects all the analyzed bands together with the symmetry of the vibrational states involved in the transitions, the band center, the observed range of J'' values for the various sub-bands, the RMS error resulting from the simultaneous least-squares analysis described below and the number of fitted and assigned lines. The $\nu_5 \leftarrow \nu_4$ band which has already been detected and analyzed [5] is included in the Table. In total, 18 vibrational bands for the $H^{12}C^{13}CD$, and 19 for $H^{13}C^{12}CD$ have been reported. Only the dominant *Q*-branch of the $\nu_4 + \nu_5 \, \Sigma^+ \leftarrow \nu_5 \, \Pi$ band was identified, the *P* and *R* branches being too weak or overlapping. The unambiguous assignment of the *Q*-branch lines was assisted by the knowledge of the energies of the states involved in the transitions from the analysis of other bands. In the region below 800 cm^{-1} the highest *J*-transitions detected were *R*(44) and *Q*(43) for $H^{12}C^{13}CD$, *R*(41) and *Q*(42) for $H^{13}C^{12}CD$ of the ν_5 fundamental band. Above 800 cm^{-1} the $2\nu_5 \, \Sigma^+ \leftarrow$ GS overtone band was the most extended, with observed transitions up to $J' = 43$ and 41 for $H^{12}C^{13}CD$ and $H^{13}C^{12}CD$, respectively.

The spectrum below 800 cm^{-1} was the first one to be analyzed. The assignment of the transitions belonging to bands previously

Table 1
Vibrational assignments and band centers, v_C, (in cm^{-1}) of the vibration–rotation bands for H^{12}C^{13}CD and H^{13}C^{12}CD.

Transition	Symmetry	v_C[a]	P, R, Q (J_{min}, J_{max})	σ ($\times 10^5$)[b]	Number fitted/assigned lines
H^{12}C^{13}CD					
(a) 100–800 cm^{-1}					
$v_4 \leftarrow$ G.S.	$\Pi \leftarrow \Sigma^+$	511.5103	P_{e-e} (2–32); R_{e-e} (0–40); Q_{f-e} (1–39)	31	104/112
$v_5 \leftarrow$ G.S.	$\Pi \leftarrow \Sigma^+$	677.8673	P_{e-e} (2–42); R_{e-e} (0–44); Q_{f-e} (1–43)	26	125/128
$v_5 \leftarrow v_4$	$\Pi \leftarrow \Pi$	166.3570	P_{e-e} (2–19); R_{e-e} (1–24); P_{f-f} (3–21); R_{f-f} (1–25);	24	76/86
$2v_4 \leftarrow v_4$	$\Sigma^+ \leftarrow \Pi$	509.0248	P_{e-e} (1–27); R_{e-e} (1–31); Q_{e-f} (8–23)	50	69/74
	$\Delta \leftarrow \Pi$	513.4702	P_{e-e} (3–20); R_{e-e} (1–23); Q_{e-f} (2–30); P_{f-f} (3–24); R_{f-f} (1–29); Q_{f-e} (2–32)	47	140/152
$v_4 + v_5 \leftarrow v_4$	$\Sigma^+ \leftarrow \Pi$	682.0082	P_{e-e} (1–27); R_{e-e} (1–27); Q_{e-f} (3–38)	35	83/89
	$\Sigma^- \leftarrow \Pi$	677.8302	P_{f-f} (1–37); R_{f-f} (1–36); Q_{f-e} (1–28)	39	88/100
	$\Delta \leftarrow \Pi$	677.4611	P_{e-e} (3–37); R_{e-e} (1–35); Q_{e-f} (2–29); P_{f-f} (3–28); R_{f-f} (1–25); Q_{f-e} (2–35)	42	174/183
$v_4 + v_5 \leftarrow v_5$	$\Sigma^+ \leftarrow \Pi$	515.6512	Q_{e-f} (1–20)	38	17/19
	$\Delta \leftarrow \Pi$	511.1042	P_{e-e} (5–21); R_{e-e}(1–29); Q_{e-f} (14–20); P_{f-f} (3–22); R_{f-f} (1–29); Q_{f-e} (4–17)	50	104/113
$2v_5 \leftarrow v_5$	$\Sigma^+ \leftarrow \Pi$	664.4116	P_{e-e} (1–36); R_{e-e} (1–35); Q_{e-f} (6–34)	35	94/98
	$\Delta \leftarrow \Pi$	681.3239	P_{e-e} (3–31); R_{e-e} (1–33); Q_{e-f} (2–20); P_{f-f} (3–36); R_{f-f} (1–33); Q_{f-e} (2–36)	33	172/183
(b) 800–1400 cm^{-1}					
$2v_4 \leftarrow$ G.S.	$\Sigma^+ \leftarrow \Sigma^+$	1020.5351	P_{e-e} (1–40); R_{e-e} (0–37)	22	77/78
	$(\Delta \leftarrow \Sigma^+)^c$	1024.9805	P_{e-e} (13–37); R_{e-e} (8–35)	42	51/53
$v_4 + v_5 \leftarrow$ G.S.	$\Sigma^+ \leftarrow \Sigma^+$	1193.5185	P_{e-e} (1–37); R_{e-e} (0–37)	25	75/75
	$(\Delta \leftarrow \Sigma^+)^c$	1188.9715	P_{e-e} (10–33); R_{e-e} (8–35)	53	49/51
$2v_5 \leftarrow$ G.S.	$\Sigma^+ \leftarrow \Sigma^+$	1342.2789	P_{e-e} (1–42); R_{e-e} (0–42)	21	83/85
	$(\Delta \leftarrow \Sigma^+)$ ^{c}	1359.1912	P_{e-e} (16–31); R_{e-e} (16–34)	54	27/36
H^{13}C^{12}CD					
(a) 100–800 cm^{-1}					
$v_4 \leftarrow$ G.S.	$\Pi \leftarrow \Sigma^+$	516.4901	P_{e-e} (2–34); R_{e-e} (0–40); Q_{f-e} (1–41)	27	114/115
$v_5 \leftarrow$ G.S.	$\Pi \leftarrow \Sigma^+$	674.1695	P_{e-e} (2–43); R_{e-e} (0–41); Q_{f-e} (1–42)	22	126/126
$v_5 \leftarrow v_4$	$\Pi \leftarrow \Pi$	157.6794	P_{e-e} (2–19); R_{e-e} (1–24); P_{f-f} (3–18); R_{f-f} (1–24);	21	75/82
$2v_4 \leftarrow v_4$	$\Sigma^+ \leftarrow \Pi$	513.8434	P_{e-e} (1–30); R_{e-e} (1–32); Q_{e-f} (9–26)	42	74/80
	$\Delta \leftarrow \Pi$	518.5725	P_{e-e} (3–21); R_{e-e} (1–25); Q_{e-f} (2–34); P_{f-f} (3–26); R_{f-f} (1–33); Q_{f-e} (3–31)	40	144/163
$v_4 + v_5 \leftarrow v_4$	$\Sigma^+ \leftarrow \Pi$	677.9093	P_{e-e} (1–27); R_{e-e} (1–23); Q_{e-f} (3–30)	30	64/78
	$\Sigma^- \leftarrow \Pi$	674.1049	P_{f-f} (1–33); R_{f-f} (1–36); Q_{f-e} (1–27)	28	84/95
	$\Delta \leftarrow \Pi$	673.7708	P_{e-e} (3–36); R_{e-e} (1–34); Q_{e-f} (2–30); P_{f-f} (3–23); R_{f-f} (1–27); Q_{f-e} (2–32)	27	166/176
$v_4 + v_5 \leftarrow v_5$	$\Sigma^+ \leftarrow \Pi$	520.2300	P_{e-e} (3–18); R_{e-e}(2–16); Q_{e-f} (3–27)	47	44/56
	$\Sigma^- \leftarrow \Pi$	516.4255	P_{f-f} (6–17); R_{f-f} (6–16);	53	18/23
	$\Delta \leftarrow \Pi$	516.0914	P_{e-e} (6–22); R_{e-e}(1–27); Q_{e-f} (14–17); P_{f-f} (4–22); R_{f-f} (1–29); Q_{f-e} (5–9)	44	77/100
$2v_5 \leftarrow v_5$	$\Sigma^+ \leftarrow \Pi$	661.0659	P_{e-e} (1–37); R_{e-e} (1–35); Q_{e-f} (7–37)	28	92/102
	$\Delta \leftarrow \Pi$	677.5693	P_{e-e} (3–31); R_{e-e} (1–34); Q_{e-f} (2–23); P_{f-f} (3–34); R_{f-f} (1–33); Q_{f-e} (2–33)	30	170/182
(b) 800–1400 cm^{-1}					
$2v_4 \leftarrow$ G.S.	$\Sigma^+ \leftarrow \Sigma^+$	1030.3335	P_{e-e} (1–38); R_{e-e} (0–38)	29	77/77
	$(\Delta \leftarrow \Sigma^+)^c$	1035.0627	P_{e-e} (10–37); R_{e-e} (8–35)	41	55/56
$v_4 + v_5 \leftarrow$ G.S.	$\Sigma^+ \leftarrow \Sigma^+$	1194.3995	P_{e-e} (1–38); R_{e-e} (0–37)	23	76/76
	$(\Delta \leftarrow \Sigma^+)^c$	1190.2609	P_{e-e} (10–34); R_{e-e} (8–35)	33	49/53
$2v_5 \leftarrow$ G.S.	$\Sigma^+ \leftarrow \Sigma^+$	1335.2354	P_{e-e} (1–40); R_{e-e} (0–40)	21	79/81
	$(\Delta \leftarrow \Sigma^+)^c$	1351.7388	P_{e-e} (15–22); R_{e-e} (17–33)	47	21/25

[a] $v_C = G^0_{v'} - B_{v'} k^2 - D_{v'} k^4 - (G^0_{v''} - B_{v''} k^2 - D_{v''} k^4)$.
[b] σ (in cm^{-1}) corresponds to the RMS value of the residuals for the various assigned lines resulting from the simultaneous fit (see text).
[c] Perturbation allowed transition.

reported [8] was accomplished extending also the *J* ranges of the various sub-branches. Subsequently, the transitions involving states not characterized were searched for. Their positions were evaluated by comparison with the analogous transitions of ^{12}C$_2$HD [3,5] and ^{13}C$_2$HD [6] isotopologues. Finally, the spectral region above 800 cm^{-1} was investigated, allowing the extension of the *J* assignment for the Σ^+ components of the first overtones and combination band [8] and the identification of perturbation allowed transitions connecting the GS to the Δe components of the same manifolds.

Initially, the transition wavenumbers for each band were fitted separately to the upper state ro-vibrational parameters, in order to check the correctness of the assignments and to extend the data set. The data were analysed using the basic Hamiltonian of a linear molecule, with centrifugal distortion corrections up to the sextic term. For the bending modes, the *l*-doubling energy contributions containing q_v and q^l_v coefficients were included in the model. The ro-vibrational energy term values are given by

$$T^0(v, J) = G^0_c(v) + B_v J(J+1) - D_v [J(J+1)]^2 \mp 1/2\{q_v[J(J+1)]$$
$$+ q^l_v[J(J+1)]^2\} \quad (1)$$

with the − and + signs related to the *e* and *f* levels, respectively, and $G^0_c = G^0_v - B_v k^2 - D_v k^4$, with G^0_v the pure vibrational term value and $k = l_4 + l_5$. The band center is defined as

$$v_C = G^0_{v'} - B_{v'} k^2 - D_{v'} k^4 - (G^0_{v''} - B_{v''} k^2 - D_{v''} k^4) \quad (2)$$

where $G^0_{v'}$ and $G^0_{v''}$ represent the purely vibrational energy of the upper and lower state.

Having identified all possible transitions in the various regions of the spectra, a simultaneous fit of all the experimental data was performed. The data set for each isotopomer contains all the rovibrational transitions listed in Table 1 and the rotational transitions measured in the millimeter- and sub-millimeter wave regions [4]. The model Hamiltonian adopted for the global analysis is the one used for ^{12}C$_2$HD [3] and ^{13}C$_2$HD [6]. The energies of the rovibrational levels of the transitions were obtained by diagonalizing the appropriate energy matrix containing the following vibration (G^0) and rotation (*F*) diagonal contributions:

$$G^0(v_4, l_4, v_5, l_5) = \omega^0_4 v_4 + \omega^0_5 v_5 + x^0_{44}(v_4)^2 + x^0_{45} v_4 v_5 + x^0_{55}(v_5)^2$$
$$+ g^0_{44}(l_4)^2 + g^0_{45} l_4 l_5 + g^0_{55}(l_5)^2 \quad (3)$$

Table 2
Spectroscopic parameters (in cm^{-1}) for H^{12}C^{13}CD and H^{13}C^{12}CD resulting from the simultaneous fit of all sub-bands involving levels up to $v_4 + v_5 = 2$[a].

Parameter	H^{12}C^{13}CD	H^{13}C^{12}CD
ω_4^0	510.5258818(578)	515.4441635(489)
ω_5^0	676.1366367(564)	672.4675880(475)
x_{44}^0	−0.1291658(280)	−0.1387044(242)
x_{45}^0	0.8265503(430)	0.7230891(358)
x_{55}^0	−2.4985993(268)	−2.4249439(225)
g_{44}^0	2.0912428(225)	2.1543718(195)
g_{45}^0	0.7288857(357)	0.8235878(300)
g_{55}^0	5.2058773(202)	5.0953053(174)
r_{45}^0	2.0889544(421)	1.9022070(324)
$r_{45}^J \times 10^3$	−0.0181602(956)	−0.0279194(872)
B_0	0.9752708273(562)	0.9671933960(484)
$\alpha_4^0 \times 10^3$	−2.409888(153)	−2.538037(130)
$\alpha_5^0 \times 10^3$	−1.452763(130)	−1.322326(116)
$\gamma_{44} \times 10^3$	0.0276600(780)	0.0315131(644)
$\gamma_{45} \times 10^3$	−0.0241946(768)	−0.0278384(691)
$\gamma_{55} \times 10^3$	0.0209485(578)	0.0208408(502)
$\gamma^{44} \times 10^3$	−0.080022(136)	−0.079994(111)
$\gamma^{45} \times 10^3$	−0.002569(218)	0.003608(199)
$\gamma^{55} \times 10^3$	−0.1193399(798)	−0.1200388(736)
$D_0 \times 10^6$	1.095686(164)	1.081457(146)
$\beta_4 \times 10^6$	0.0319551(817)	0.0340680(669)
$\beta_5 \times 10^6$	0.0140976(626)	0.0123235(590)
$q_4^0 \times 10^3$	4.313444(203)	4.201655(172)
$q_5^0 \times 10^3$	3.360873(407)	3.326577(384)
$q_4^J \times 10^6$	−0.036047(139)	−0.035469(113)
$q_5^J \times 10^6$	−0.020657(109)	−0.019941(102)
$q_{44} \times 10^3$	0.036813(200)	0.033417(170)
$q_{45} \times 10^3$	−0.003740(227)	−0.004575(211)
$q_{54} \times 10^3$	0.011155(105)	0.0133556(972)
$q_{55} \times 10^3$	0.050549(402)	0.049875(378)
$\rho_4^0 \times 10^9$	−4.617(410)	−0.794(334)
$\rho_5^0 \times 10^9$	−5.291(193)	−4.158(192)
Number of fitted/assigned data	1617/1722	1613/1754
St. dev. of the fit $\times 10^4$	3.8	3.2

[a] Estimated uncertainties (1σ) are given in parentheses in units of the last figure quoted.

$$F(v_4, l_4, v_5, l_5) = [B_0 - \alpha_4 v_4 - \alpha_5 v_5 + \gamma_{44}(v_4)^2 + \gamma_{45} v_4 v_5 + \gamma_{55}(v_5)^2$$
$$+ \gamma^{44}(l_4)^2 + \gamma^{45} l_4 l_5 + \gamma^{55}(l_5)^2][M - k^2] - [D_0 + \beta_4 v_4$$
$$+ \beta_5 v_5 + \delta_{44}(v_4)^2 + \delta_{45} v_4 v_5 + \delta_{55}(v_5)^2 + \delta^{44}(l_4)^2$$
$$+ \delta^{45} l_4 l_5 + \delta^{55}(l_5)^2][M - k_2]^2 + [H_0 + h_4 v_4$$
$$+ h_5 v_5][M - k^2]^3 \quad (4)$$

Vibrational and rotational l-type resonances are expressed by off-diagonal matrix elements [3] containing the following parameters:

$$r_{45} = r_{45}^0 + r_{445}(v_4 + 1) + r_{455}(v_5 + 1) + r_{45}^J M) \quad (5)$$

$$q_t = q_t^0 + q_{tt} v_t + q_{tt'} v_{t'} + q_t^J M + q_t^k (k \pm 1)^2 \quad (6)$$

$$\rho_t = \rho_t^0 + \rho_{tt} v_t + \rho_{tt'} v_{t'} + \rho_t^J M \quad (7)$$

and ρ_{45}^0, with $M = J(J + 1)$, t, $t' = 4$ or 5.

The weights of the experimental data were chosen proportional to the inverse of their squared estimated uncertainties. An uncertainty of 2×10^{-4} cm^{-1} was given to wavenumbers of the IR transitions. An uncertainty of 1×10^{-4} cm^{-1} was attributed to the $v_5 \leftarrow v_4$ transitions while that of the pure rotational lines was set to 1×10^{-6} cm^{-1} (30 kHz). Finally, all the transition wavenumbers that differed from the corresponding calculated values by more than 5 times their uncertainties were excluded from the data set in the final cycle of the analysis.

In total, 1617 (1613) line wavenumbers were considered in the final cycle of the global fit for H^{12}C^{13}CD (H^{13}C^{12}CD). The number of lines excluded from the fit, because they were overlapping or exceeding the chosen limit for rejection, was 105 (141) for H^{12}C^{13}CD (H^{13}C^{12}CD). No evident perturbation was spotted by anomalies in the line positions or intensities The standard deviation of the fit equal to 3.8×10^{-4} cm^{-1} (3.2×10^{-4} cm^{-1}) for H^{12}C^{13}CD (H^{13}C^{12}CD) is about 1.5 times the estimated experimental precision for the IR lines.

The same set of 32 parameters, which are listed in Table 2, were obtained for both isotopomers. They are all well-determined, the only exception being ρ_4^0 of H^{13}C^{12}CD, whose value is about 2.5 times its uncertainty. The values of corresponding parameters are very similar, in magnitude and sign, apart from the higher order constants γ^{45} which have opposite signs and ρ_4^0, whose values differ by about a factor of 5. The values of B_0 and D_0 obtained in the present analysis are within 1σ as compared with those obtained from ground state combination differences [8] or from pure rotational transitions [4]. No comparison can be made with the other spectroscopic parameters in [8] since: (a) they were derived from a band by band analysis, (b) only Σ^+ states involving excitation of two quanta of the bending modes were analyzed. The two sets of parameters in Table 2 can be compared with the corresponding ones of ^{12}C$_2$HD [3] and ^{13}C$_2$HD [6], whose analysis considered bending states up to $v_4 + v_5 = 3$. As expected, they show strong similarities although a precise comparison cannot be made since the parameters obtained in the present work were derived from a smaller set of data involving bending states up to $v_4 + v_5 = 2$. As a consequence, a number of higher order dependences of the vibrational, rotational and l-resonance constants could not be determined. Nevertheless, all the leading parameters of H^{12}C^{13}CD and H^{13}C^{12}CD have values intermediate between those in [3,6]. In particular, the values of the rotational, B_0 and D_0, l-resonance, g_{55}^0, q_4^0, q_5^0, r_{45}^0, and vibrational, ω_5^0 and x_{55}^0 constants of H^{12}C^{13}CD are close to those in ^{12}C$_2$HD [3] while the corresponding parameters of H^{13}C^{12}CD are similar to those in ^{13}C$_2$HD [6]. On the contrary, the vibrational constants ω_4^0 and g_{44}^0 behave just the opposite. We

Table 3
Vibrational term values, G_c^0, (in cm^{-1}) of the observed k-substates in ^{12}C$_2$HD, H^{12}C^{13}CD, H^{13}C^{12}CD, and ^{13}C$_2$HD[a].

v_4	v_5	Symmetry	l_4	l_5	^{12}C$_2$HD	H^{12}C^{13}CD	H^{13}C^{12}CD	^{13}C$_2$HD
1	0	Π	± 1	0	518.3814	511.5103	516.4901	509.5852
0	1	Π	0	± 1	677.8077	677.8673	674.1695	674.2363
2	0	Σ^+	0	0	1033.9353	1020.5351	1030.3335	1016.8514
2	0	Δ	± 2	0	1038.7208	1024.9805	1035.0627	1021.2523
1	1	Δ	± 1	± 1	1195.7494	1188.9715	1190.2609	1183.4615
1	1	Σ^-	−1	1	1196.1630	1189.3406	1190.5951	1183.7444
1	1	Σ^+	1	−1	1200.4981	1193.5185	1194.3995	1187.4126
0	2	Σ^+	0	0	1342.2264	1342.2789	1335.2354	1335.3085
0	2	Δ	0	± 2	1359.0490	1359.1912	1351.7388	1351.8993

Upper signs of l_4 or l_5 refer to 'e' states; lower signs refer to 'f' states.
[a] Term values, G_c^0, are expressed as $G_v^0 - B_v k^2 - D_v k^4$ (see text).

recall that the value of x_{44}^0 in $^{13}C_2HD$, 0.010493 cm^{-1} [6], is one order of magnitude smaller and opposite in sign with respect to that in $^{12}C_2HD$, −0.143558 cm^{-1} [3]. The corresponding constants in Table 2 are both close to the latter value.

Table 3 lists the vibrational term values G_c^0 of the observed k-substates for the studied molecules together with the corresponding values for $^{12}C_2HD$ [3] and $^{13}C_2HD$ [6]. The comparison of the vibrational term values for the trans and cis bending excited states exhibits the same trend described above for the spectroscopic parameters, i.e. they are different for the two bending coordinates. A more meaningful comparison could be made by taking into account the zero point energies for each isotopologue.

4. Conclusions

The infrared spectrum of $H^{12}C^{13}CD$ and $H^{13}C^{12}CD$ has been recorded in the 450–1450 cm^{-1} spectral interval. All the bending fundamental bands and a number of overtone, combination and hot bands involving excitations of the bending modes up to $v_4 + v_5 = 2$ have been detected. About 1750 assigned transitions were analyzed in a global rotation−vibration fit for each isotopomer, yielding a set of 32 spectroscopic parameters. The analysis of the stretching−bending combination bands and overtones present in the higher energy region has been undertaken to complete the spectroscopic characterization of the two isotopomers.

Acknowledgments

Appendix A. Supplementary material

The supplementary data for this article, containing the lists of transitions assigned to the bands of $H^{12}C^{13}CD$ and $H^{13}C^{12}CD$, together with the corresponding (observed–calculated) values obtained using the parameters in Table 2, are available on ScienceDirect (www.sciencedirect.com) and as part of the Ohio State University Molecular Spectroscopy Archives (http://msa.lib.ohiostate.edu/jmsa_hp.htm). Supplementary data associated with this article can be found, in the online version, at doi:10.1016/j.jms.2011.06.006.

References

[1] A. Coustenis, D.J. Jennings, A. Jolly, Y. Benilan, C.A. Nixon, S. Vinatier, et al., Icarus 197 (2008) 539–548.
[2] A. Jolly, Y. Benilan, E. Canè, L. Fusina, F. Tamassia, A. Fayt, S. Robert, M. Herman, J. Quant. Spectrosc. Rad. Transf. 109 (2008) 2846–2856.
[3] L. Fusina, E. Canè, F. Tamassia, G. Di Lonardo, Mol. Phys. 103 (2005) 3263–3270.
[4] G. Cazzoli, C. Puzzarini, L. Fusina, F. Tamassia, J. Mol. Spectrosc. 247 (2008) 115–118.
[5] A. Predoi-Cross, M. Herman, L. Fusina, G. Di Lonardo, Mol. Phys. 109 (2011) 559–563.
[6] L. Fusina, F. Tamassia, G. Di Lonardo, A. Baldan, Mol. Phys. 107 (2009) 2119–2126.
[7] S. Ghersetti, A. Baldacci, S. Giorgianni, H. Russell, R.H. Barnes, K. Narahari Rao, Gazz. Chim. It. 105 (1975) 875–900.
[8] L. Fusina, E. Canè, F. Tamassia, G. Di Lonardo, Mol. Phys. 105 (2007) 2321–2325.
[9] R.E. Colborn, K.P.C. Volhardt, J. Label, Compd. Radiopharm. 20 (1983) 257–267.
[10] G. Di Lonardo, A. Baldan, G. Bramati, L. Fusina, J. Mol. Spectrosc. 213 (2002) 57–63.
[11] R.A. Toth, J. Opt. Soc. Am. B 8 (1991) 2236–2255.
[12] G. Guelachvili, K. Narahari Rao, Handbook of Infrared Standards, Academic Press, San Diego, 1986.
[13] G. Di Lonardo, A. Baldan, L. Fusina, in preparation.